

# FEA Simulations for Comparison to Thermal Data Obtained from Vehicle Testing on the Grossglockner High Alpine Road

Wren Stewart, Suarez Fernando, Sims, Richard\*

EURAC Poole Ltd, UK [A member of the MAT Foundry Group Ltd]

Keywords: *thermal analysis, ventilated brake rotor, finite element analysis, thermal loading, alpine testing*

## Abstract

With an increasing stringency upon carbon emissions throughout the automotive sector, mass reduction strategies for components and assemblies are being brought evermore closely into focus. For the safety-critical braking sub-assembly, mass reductions are competitively requisite and cannot negate any safety or performance characteristics. This is where the use of increasingly comprehensive analytical methods, such as Finite Element Analysis (FEA) has yielded merits. Presented is a methodology for determining a suitable simulation model for the prediction of thermal affects for brake rotors, in particular those induced under the operational conditions during a descent of Grossglockner Alpine Pass (GAP). Under these driving conditions, the sustained braking subjects the rotor to considerably higher levels of heat flux, and hence the notable use of the GAP in automotive testing.

Thermal FEA simulations were conducted alongside experimental procedures, closely matching the vehicle dynamics in order to compare the thermal behaviour. Yielding a high degree of correlation, these simulations provided the opportunity to realise a design procedure that eliminated the need for native experimental data. This offered demonstrative validation of untested rotor geometries at an early stage in the design. Presented is a simplified thermal study of a complex transient system where a single-body approach was used. Necessary simplifications were utilised and this included the omission of some complex dynamic phenomena e.g. turbulent cooling. These reductions in complexity provided a means to create a procedural basis from which to develop. Such models will be subjected to sustained refinement and validation against additional data sets to improve the prediction efficacy.

## Introduction

Brake rotors are individually designed to suit the particular application and vehicular requirements. A plethora of specific design criteria exist but thermal behaviour is among the more important. The rotor ultimately has to meet the thermal requirements of the braking application, whereby the vehicles kinetic energy (KE) and potential energy (PE) are largely converted into heat at the pad/rotor frictional interface. The resulting temperature increase must not adversely affect the operational capability of the rotor, and thus it must be designed to manage such changes. Secondly the rotor must meet the geometric requirements of the vehicle, ensuring that the shape and size are suitable for the wheel positioning, mounting and calliper alignment. The air flow schemes around the rotor that provide the cooling are also of particular importance and shall dictate certain geometries of the rotor, in particular the topology of the vanes. These cooling vanes bridge the inboard and outboard braking rings and

typically follow a radial pattern as seen in Fig. 1. Certain driving scenarios such as an emergency stop or inclined braking will subject the rotor to larger changes in temperature, along with increased subsequent stresses and greater deformations.



**Figure 1: Cut section of a ventilated brake rotor.**

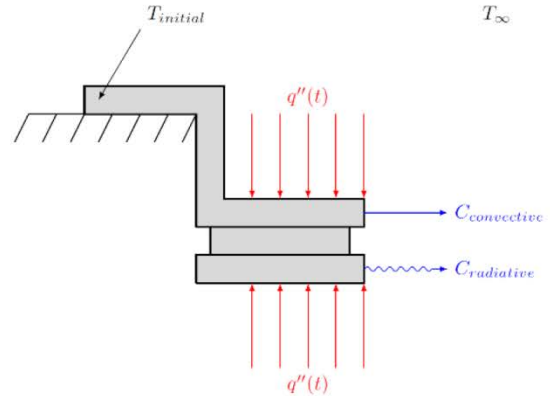


**Figure 2: Free Body Diagram (FBD) with constraints and loadings.**

The use of FEA simulations coupled with Computational Fluid Dynamics (CFD) analysis, can assist in the systematic design process and validate or disregard design iterations. This will take the final component through comprehensive testing and approval stages with substantially reduced costs and lead times. It is not something that should be relied upon solely, but in accompaniment with experimental failure testing, a suitable product should emerge. It is becoming increasingly common for customers to request preliminary simulation work to be carried out at the quotation stage, necessitating the use of FEA simulations in the commercial market.

Four experimental procedures were conducted and compared to subsequent equivalent FEA simulations. The aim was to create and validate a simulation methodology that could be used as a design tool. This was achieved by selecting an experimental velocity profile that most suitably characterised a descent of GAP. Second to this, simulation criteria such as cooling parameters were defined. Such a system would be integrated into the overall analytical design of the component. Utilisation of this practice during the initial design phase of the component would assist in the validation or dismissal of concepts. Through studies of the literature and existing work, simple simulations were carried out. These developed into more scientifically rigorous and comprehensive studies of the braking mechanism which led to an experimental phase of work. Finally results were analysed and compared until a valid method was obtained, presenting an appropriate methodology for the thermal validation of geometric designs.

## Theory

The presented mathematical braking model, is a simplification of a complex process in which many variables and phenomena are present. It is important however, to accurately calculate the energy that is added to the braking system during deceleration using kinematics; the validity of subsequent results will be critically dependent upon these values, considering most of this energy will be transmitted to the tribological system. In reality, the vehicle motion is governed by braking, cornering, accelerations and variations in road profile. A relatively small fraction of the energy from the vehicle motion is not converted to heat upon braking. Sources of loss from the kinematic motion of the vehicle include:

- 1. Loss of tyre adhesion with road surface.**
- 2. Tyre deformation along with the associated pressure change in the tyre.**
- 3. The elastic deformation within the springs and bushes of the suspension system.**
- 4. The minimal but present deformation in the structure of the vehicle.**
- 5. The force of aerodynamic drag upon the vehicle.**
- 6. Passenger displacement within the vehicle under severe braking instances.**
- 7. Losses through the compressibility of hydraulic brake fluid.**
- 8. Noise and vibrations generated from frictional interactions.**

This generated heat energy will be transmitted away from the rotor, towards contiguous and neighbouring components within the braking system. These sub-assembly components include: brake pad, pad backing-plate, hold-down clip, calliper, hydraulic fluid, mounting hub and wheel section. The primary heat transfer mechanisms are convective and radiative cooling, the former of which uses circulating air flow within the rotor vents and wheel arch. Emissivity values obtained experimentally by Tirovic (1) were found to range from 0.2 to 0.9 and recommendations were made to use an average value of 0.55. The emissivity value obtained from (4) for grey cast iron was 0.44 (for recently machined surfaces). An emissivity value of 0.55 was chosen for simulation studies. The employed mathematical model assumed a straight road of constant incline, with an equal distribution of mass over the left and right sides of the car. Corners were only considered for their reduction in velocity, rather than the resulting asymmetrical distribution of mass over left and right sides of the car. Forces of aerodynamic drag were neglected but will provide marginal assistance in the deceleration of the vehicle.

The rotor was modelled as an individual component in a way which did not consider the calliper assembly, pads or wheel. The rotor was constrained via the surface of the hub and heat fluxes were applied to the two frictional annuli as shown in Fig. 2. The radial symmetry of the component lends itself to the use of a geometric symmetry condition, in which only a sector of the rotor was modelled whilst retaining the characteristics of the entire rotor. Fig. 3 shows the geometry that was used. The heat flux was applied to a non-rotating component, such that the thermal input was not concentrated to any one area. Instead the heat flux was applied with a uniform distribution over the entire swept area. In reality, a non-uniform distribution of heat flux would revolve around the rotor, with an area closely representing the pad contact envelope.

The braking instances were modelled over a finite time period which was designated by the time between  $t_1$  and  $t_2$ . The approximation was made for the deceleration due to braking  $ab$ , to be constant over this time. The act of braking reduced the velocity of the vehicle from  $v_1$  to  $v_2$ .

The time-evolution of heat flux was represented by a ramp change from zero heat flux at  $t_1$  to a maximum heat flux  $q_{max}$ , at a time  $t_{max}$ , which was calculated as 10 percent of the total braking duration, after which, a ramp change down to zero heat flux at  $t_2$  as shown in Fig. 4.



Figure 3: An 18 degree sector of meshed geometry.

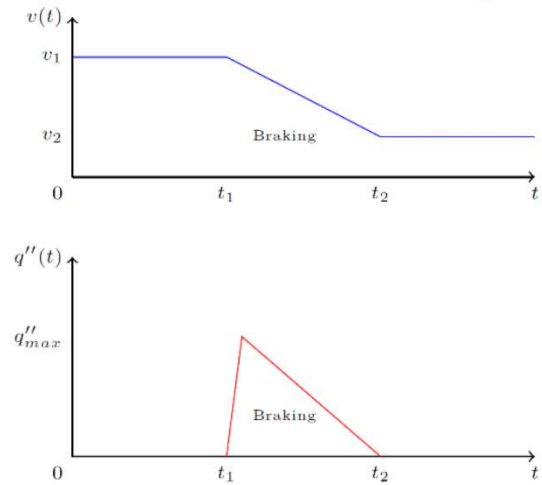


Figure 4: Heat flux and velocity w.r.t. time.

It is necessary to determine the effective mass for which each respective brake is responsible. This apportionment of mass over the front and rear axles is critical in determining suitable values of flux for any particular braking instance. With the assumption of straight roads and no corners, it follows that the left and right rotors receive equal amounts of heat energy. The maximum possible deceleration without tyre slippage, where the tyre adhesion coefficient  $\psi$ , is 0.8 (2) is given by  $ab_{max} = \psi g$ . The height  $h$ , of the centre of gravity is taken as  $0.2L$ . The longitudinal load transfer is the change in reactionary forces during braking and will be used to for the determination of equivalent mass braked.

### Calculation of a Dynamic Mass Balance

Thermal loading of the rotor considers KE and GPE. Both components required the equivalent mass braked by a rotor and this was subject to change based upon vehicle deceleration as indicated in Fig. 5. The apportionment of loading over the front and rear axles is important because it will dictate the thermal loading to those respective systems. The vehicle is assumed to travel down the incline with a constant velocity and the braking force acts in the opposite direction to the vehicle motion. Initiation of braking during the descent, established deceleration forces on the vehicle that distributed reactionary forces over the front and rear axles. This dynamic balance of “mass”, which governs the perpendicular loading over the front and rear axles, considering the braking forces was calculated as a function of inclination angle  $\theta$  and the braking deceleration  $ab$ . Outlined below is the formulation of the dynamic mass balance,

$$\Sigma F_x = -ma \quad (1)$$

$$\Sigma F_y = 0 \quad (2)$$

$$\Sigma M_z = 0 \quad (3)$$

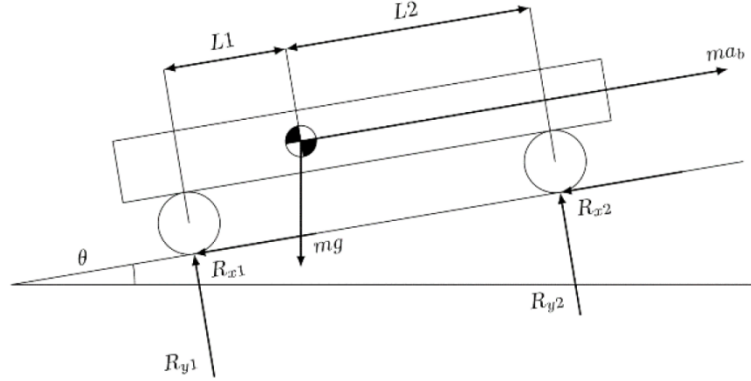


Figure 5: FBD of the vehicle at the initiation of braking on an incline of  $\theta$  and with a deceleration of  $a_b$ .

$$\Sigma F_x = -ma = R_{x2} + R_{x1} + mgsin\theta \quad (4)$$

$$\Sigma F_y = 0 = R_{y2} + R_{y1} - mgcos\theta \quad (5)$$

$$\Sigma M_z = 0 = R_{y1}L1 + R_{x1}h + R_{x2}h - R_{y2}L2 \quad (6)$$

Resulting in,

$$R_{y1} = mgcos\theta - R_{y2} \quad (7)$$

$$R_{x1} = -ma - R_{x2} - mgsin\theta \quad (8)$$

Perpendicular reactionary forces are described by the following:

$$R_{y1} = mgcos\theta - \frac{mg}{L} \left( L1cos\theta - h \left( \frac{a}{g} + sin\theta \right) \right) \quad (9)$$

$$R_{y2} = \frac{mg}{L} \left( L1cos\theta - h \left( \frac{a}{g} + sin\theta \right) \right) \quad (10)$$

Dynamic weight balances  $\xi_f$  and  $\xi_r$  over the front and rear axles were calculated using force and moment equilibria. The equivalent mass braked by a single rotor is half of that braked by the axle. Now that the dynamic mass balance is determined, it is used to calculate the braking energy involved in a single braking instance. This study will focus on the front brake only. The distance travelled along the slope  $s$ , is found from simple dynamics,

$$s = v_1 t_b + 0.5at_b^2 \quad (11)$$

Braking energy  $E_b$ , consists of the GPE and KE from the vehicle motion. The change in height  $\delta h$  during any braking instance is found using the values of  $v_1$  and  $v_2$  at times  $t_1$  and  $t_2$  respectively. The vertical component for use in the GPE calculation is found trigonometrically considering a road incline of  $5.5824^\circ$  over the entire length. Assuming  $a_b$  to be constant,

$$E_b = (m_{b\,f\,disc} g \delta h) + 0.5(k m_{b\,f\,disc})(v_1^2 - v_2^2) \quad (12)$$

Where the rotational inertia factor  $k$ , is 1.1 (3) and it is assumed that the apportioned mass used for the GPE component is the same as used in the KE component. Brake duration is  $t_b$  and braking power  $P_b$  is,

$$P_b = \frac{E_b}{t_b} \quad (13)$$

The heat flux is the rate of heat energy transfer into the rotor over the entire swept area. The frictional annulus is the region bound by the inner and outer diameters swept by the pad and only half of the contact area  $A_f$ , in a dual-pad system. Where the heat flux  $q''$ ,

$$q'' = P_b / A_f \quad (14)$$

The  $q''$  values are calculated for each braking event throughout the driving scenario using the experimental values of velocity; calculated linear deceleration and mass balance [see Fig. 6 fo]. This data along with  $t_1$ ,  $t_2$  and  $t_{max}$  can be tabulated and used to make the final time-amplitude history of heat flux, as shown in Lis. 1. The heat flux input is taken almost entirely into the rotor as opposed to the pad and factor of 0.99 was used (7). Time of maximum heat flux  $t_{max}$  is,

$$t_{max} = t_1 + ((t_2 - t_1)/10) \quad (15)$$

Time	Heat Flux
0	0
17.05	0
17.55	0.129284418
22.01	0
30.97	0
31.417	0.169190897
35.44	0
...	...

Listing 1: Partial heat flux amplitude for two braking instances only.

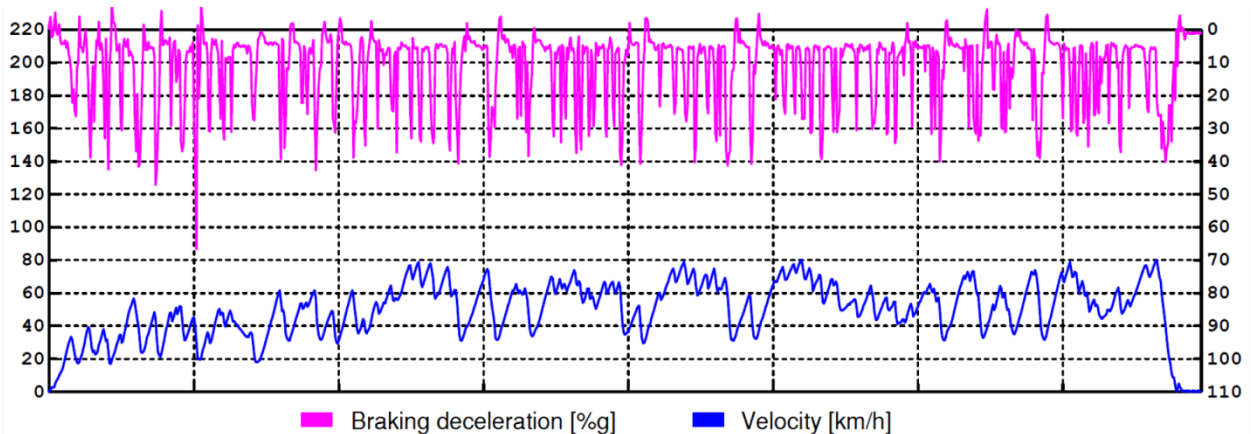


Figure 6: Example velocity and braking deceleration profiles for a GAP descent.

A loss factor of 0.9 was introduced for thermal energy transferred to the rotor and accounted for any losses at the frictional annuli. Energy not directly converted to heat at the interface can be accounted for by noise, deformation of rotor, deformation of pad, braking-assembly movement and third body frictional products. The latter provides an intermediary layer between pads and rotor, consisting of gas and particles and is formed from high temperature reactions (6).

A two phase cooling scheme was adopted in which two film coefficients were used, one for the descent and another for the static cooling. This additional static cooling curve helps to further validate the simulated cooling behaviour by demonstrating an adequate correlation. The average of the mean velocities obtained, provided a value of 50 km/hr and so in accordance with data recorded by Tirovic in (8), a suitable value was selected. Film coefficients for the descent and stationary conditions were  $20 \text{ Wm}^{-2}\text{K}^{-1}$  and  $5 \text{ Wm}^{-2}\text{K}^{-1}$  respectively.

### **Grossglockner**

Grossglockner at 2558 m, is an alpine road in Austria that is routinely used for the testing of brake rotors among other components. The nation's highest road presents automotive manufacturers with the opportunity to test under extreme driving conditions and for continual heat input to be applied the rotor. The selected route begins at Edelweißspitze (coordinates 47.123890, 12.831235) and ends at (47.142790, 12.814140) having travelled 14.4 km and descended to an altitude of 1118 m. The inclination taken from this data was 5.5824 degrees. In one example experiment a VW Tiguan braked 107 times over 954 s and reached speeds of 80 kmhr-1.

### **Experimental Data**

Roulunds Braking were responsible for test procedures and retrofitting four road vehicles with data acquisition and recording equipment, see Figs. 7-8. To create testing conditions with the highest possible thermal loadings, the four vehicles were equipped with water containers to act as occupants and sand ballast to mimic fully-laden load conditions. Each of the four vehicles made an experimental descent of the GAP. Steel wheels were used to reduce the cooling air flow into the brake rotor to observe conditions in which the rotor temperatures will be the highest. For each descent an on-board computer recorded the following values:

- 1. Temperature of all four rotors as a function of time, recorded from the centre of the frictional surface using an embedded thermocouple.**
- 2. The temperature of the hydraulic fluid in the subsystems for each respective rotor.**
- 3. Ambient initial temperatures are recorded.**
- 4. Velocity of the vehicle with respect to time.**
- 5. Braking deceleration with respect to time.**
- 6. Brake pressure with respect to time.**
- 7. Brake pedal travel with respect to time.**



Figure 7: An interior view showing instrumentation.



Figure 8: Thermocouple setup for recording data.

Front brakes were exclusively the focus of the current study considering the larger contribution to the reduction in velocity that they provide. To simulate the thermal loading in a computational environment, the experimental data was used to map a suitable time-amplitude history for the heat flux. The experimental data coupled with suitable initial vehicle conditions yielded simulation results that were in high correlation to the experimental data.

Property	Value	Source
Vehicle Mass	2263kg	Experimental Data
Vehicle Weight	22,000N	
Mass over front axle	1167kg	Experimental Data
	1096kg	Experimental Data
	52%	
	2.604 m	(5)
	1.686 m	(5)

Table 1: Example vehicle data from the VW Tiguan used in testing.

For each braking event the start  $t_1$ , and end times  $t_2$ , were taken from each peak in the hydraulic fluid pressure data. These times were then used to identify the corresponding values of velocity at the start  $v_1$ , and end  $v_2$ , of each braking event from the velocity data. This allowed a constant linear deceleration to be calculated over the braking event. This was then used to obtain the distance travelled during the braking event, which if coupled with the assumption of a constant incline, can be used to find a drop in elevation for each braking event. The values were then used to create a flux amplitude history to apply to the appropriately constrained and cooled FEA model.

#### Simulation Procedure

ABAQUS was utilised to simulate the thermal and mechanical behaviour of the brake rotor during operation. It was used to apply the necessary loadings to the brake rotor and to review the resulting behaviour. A simulation that matched the descent characteristics was conducted for each of the four experiments. Parallelisation of cores was used to better distribute the computational load. For every time increment 44,454 equations were required for these particular meshing parameters, collectively computing a total of  $2.31E+10$  floating point operations. To increase computational efficiency a small sector of this rotor was modelled. This was based upon the degree of rotational symmetry i.e number of radial vanes. The material data assigned included density and temperature dependant values for elastic behaviour, thermal expansion, plastic behaviour, specific heat and thermal conductivity. Thermal



loading applied to the rotor was characterised by a surface heat-flux and governed by a flux amplitude history. The values for which were tabulated as decimal equivalents using a maximum flux value, along with the associated times of each braking event, see Fig. 6.

The radiative cooling was defined using surface radiation with an emissivity of 0.55 and a constant ambient sink temperature of 293.15 K. The radiative cooling scheme was applied to all surfaces of the rotor with the exception of the symmetry condition and mounting faces. The convective cooling of the rotor was approximated with a surface film condition with a coefficient of  $5 \text{ Wm}^{-2}\text{K}^{-1}$ . A constant nodal temperature was applied for initial conditions. The mounting surface was constrained with the boundary conditions (BC),  $U1 = U2 = U3 = UR1 = UR2 = UR3 = 0$ , dictating that no nodes circumscribed by the mounting surface could move or rotate. Another BC constrained the rotor from deformations that would invalidate the scheme of rotational symmetry.

Algorithmic mesh generation was improved and made less prone to failures through the reduction of surface quantities. These were absorbed into larger topologies that still reflected the 3D geometry but could be more readily divided up into mesh elements. An example illustration of the meshing regime can be seen in Fig. 3 and details are provided in Tab. 2.

Property	Value
Elements	52,142
Nodes	111,113
Global See Size	0.002m

Table 2: Meshing criteria.

## Results

Results obtained from the methodology outlined above provided high levels of correlation and a low spread of values. The accumulation of slight inaccuracies in the heating and cooling modes over the course the simulated time-step is considered as a potential source of deviation. Uneven temperatures of the braking faces can be seen in Figs. 9-10. The absence of material within the vane cavity could account for this, because less mass is present and it reduces the extent of conductive heat transfer. A surface oxide that is generated on the frictional surfaces at elevated temperatures, changes the frictional scheme to a tribo-oxidative one and may account for a greater extent of deviation (9).

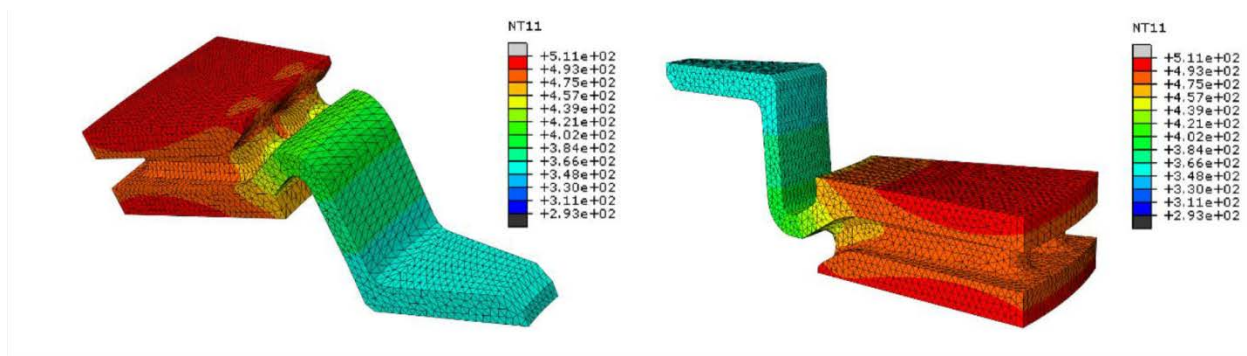
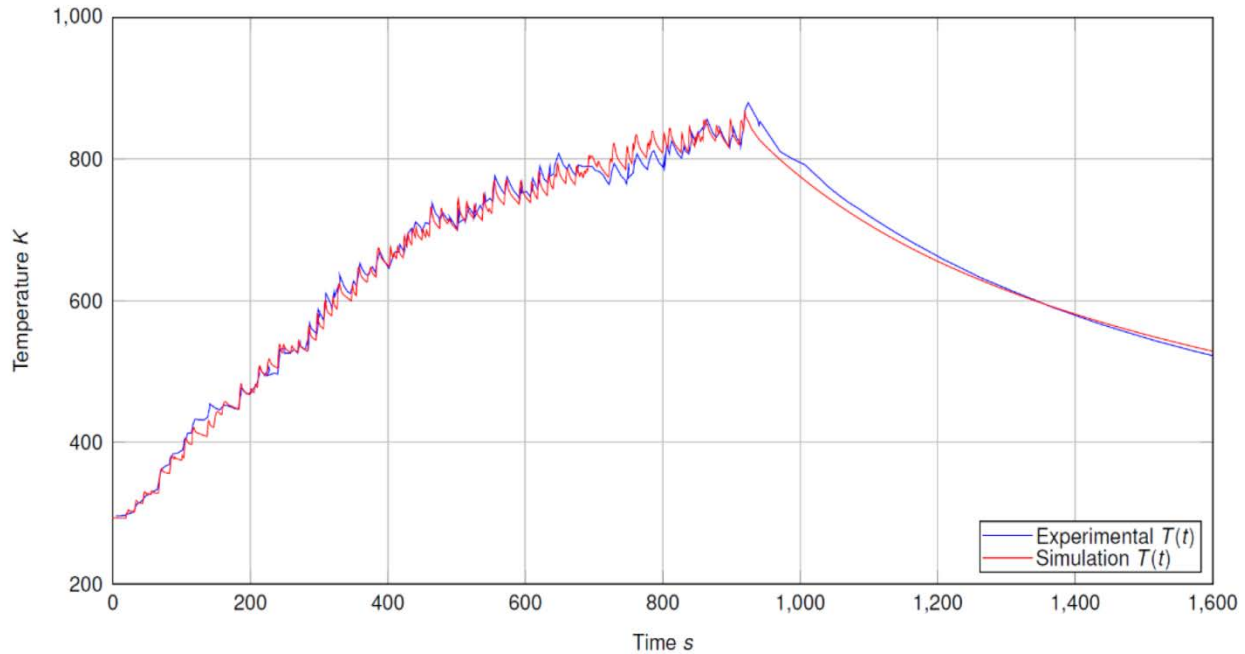


Figure 9: Nodal temperature contours at  $t = 655 \text{ s}$ . Figure 10: Additional orientation at  $t = 655 \text{ s}$ .



**Figure 11: Comparison of the simulated and experimental local temperature values at the centre of the pad from the VW Touran.**

These highly correlated simulation results led onto the next phase of the project where a generic velocity profile was to be chosen. For use as a design validation tool for untested rotor geometries, a procedure was established that required a standard experimental velocity profile for a general descent. This eliminated the necessity for new experimental data when qualifying untested rotor geometry. This was made possible from the excellent correlation of the simulation results with the experimental data as shown in Fig. 11. To identify which experimental velocity profile was the most suitable for use in a simulation as a general design tool, the experimental temperature results of the vehicle test were compared to the temperature results of four simulations, each simulation using a different one of the four experimental velocity profiles and vehicle parameters that matched that particular experiment. Each vehicle was compared to one simulation and three hybrid simulations [see Fig. 12]. Obviously the simulated temperatures will be most similar to the experimental temperatures when the simulation uses the native experimental velocity profile and so were omitted from comparisons. This process was repeated for all four vehicles in the same manner and compared by considering  $T_{MAX}$ , details of which are included in Tab. 3. An example of the data sets compared for the VW Touran for clarity:

- 1. VW Touran simulation and experimental.**
- 2. VW Touran - VW Sharan Hybrid simulation in which the vehicle data from the Touran and the velocity profile from the Sharan are used.**
- 3. VW Touran - VW Passat Hybrid in which the vehicle data from the Touran and the velocity profile from the Passat are used.**
- 4. VW Touran - VW Tiguan Hybrid in which the vehicle data from the Touran and the velocity profile from the Tiguan are used.**

These comparisons finally led to the most suitable experimental velocity profile being selected.

Vehicle	VW Touran 2.0TDI	VW Sharan 2.0TSI	VW Passat 2.0TSI	VW Tiguan 2.0
Total Mass Kg	2290	2580	2270	2263
Mass (Static) %	50.65	50.35	50.22	52.00
Wheelbase m	2.678	2.919	2.712	2.604

**Table 3: Details of the vehicles used during the experimental procedures.**

The maximum simulated temperatures of the component during the descent were compared. This simple comparison was effective as it illustrated the behaviour nearing the end of the descent, enveloping any inaccuracies which may accumulate over the course of the many braking instances. The simulations that made use of the original velocity profiles for the vehicle presented a high level of accuracy, ranging from 1.5 % to 7.1 % with a mean of 4.5 %.

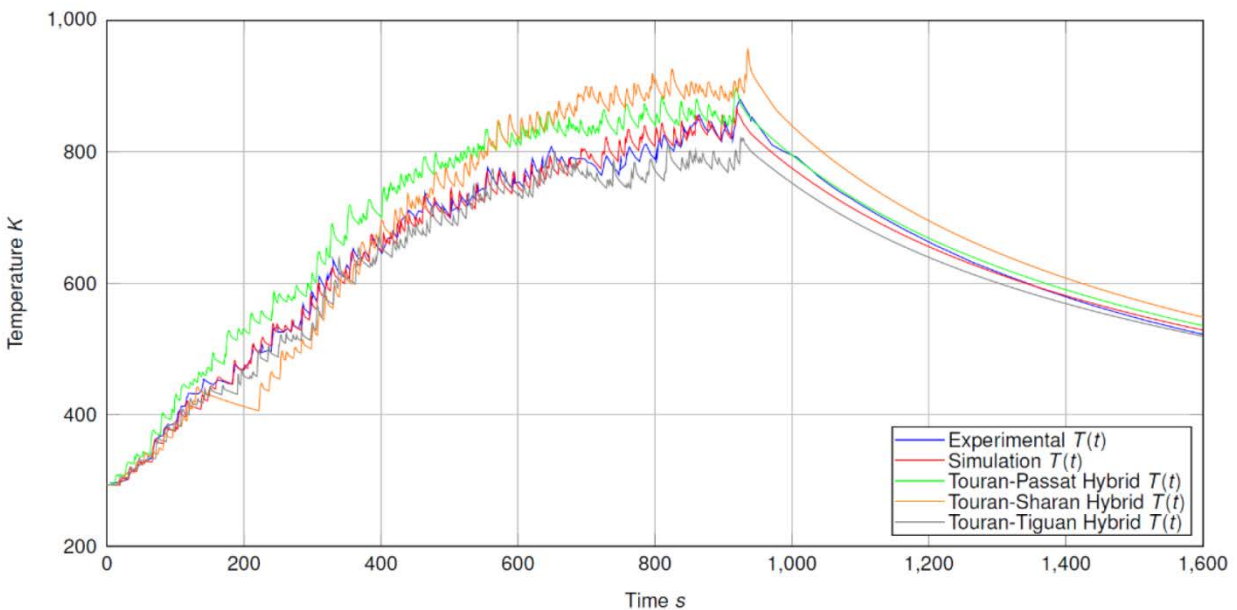


**Figure 12: VW Touran simulated, where the experimental temperature profile was compared with simulated temperature profiles generated using all four vehicle velocity profiles.**

### Chosen Velocity Profile

The VW Passat experimental velocity profile was selected because when used in the hybrid simulations it offered the most suitable correlation of simulated and experimental  $T_{MAX}$  values. Each comparison between experimental temperatures and those of the 3 respective hybrid simulation yielded a percentage error in  $T_{MAX}$ . An average of these error percentages was used as a final ranking of accuracy. The VW Passat experimental velocity profile provided a minimum deviation of 3.0 %, maximum deviation of 6.9 % and a mean of 4.8 %. Linear proportionality of mass in the braking energy (KE) could be seen in the comparisons when normalised. This validated a side hypothesis that the larger deviations in temperature, were in part, the result of greater mass differences between the vehicle that provided the velocity profile (VW Passat) and that used during experimental testing. Far lower deviations were observed if the maximum simulated temperatures were normalised in a way that presented the data without the influence of vehicle mass.

## Conclusions

The present work considers simulation techniques derived from experimental data sets. These are applied to assessing the behaviour of ventilated rotors during sustained braking and high thermal loading. Whilst this method offers reasonable projections for the thermal loading upon the rotor, it is not without limitations. For true component verification, it is also necessary to experimentally validate the final iteration of any design. This implementation of numerical analysis will assist in the reduction of development times and costs, avoiding the initial appropriations for the production of small test batches. Reducing the number design iterations before an effective component is realised, will shorten the time to market and offer increased design efficiency.

Although the negative inclination of the road was in fact particularly uniform, there were sections of the road that had a positive incline. Thus in accordance with energy conservation, the equations that govern the mass balance across both front and rear axles should account this. This would require a coordinate based profile of the road that could be used to facilitate the adjustment in the polarity of the GPE component. Far from straight, the meandering alpine descent appears to take on a left-right bias, which is illustrated in the predominance of higher rotor temperatures on the right side of the vehicle [see Fig. 14]. This observation was influential in choosing the data sets from a rotor under more rigorous thermal loading. The temperature profile of the frictional contact area is not uniform and so one single temperature reading could not offer a perfect illustration of the thermal behaviour. Additionally the presence of hot spots or hot rings could adversely affect the data.

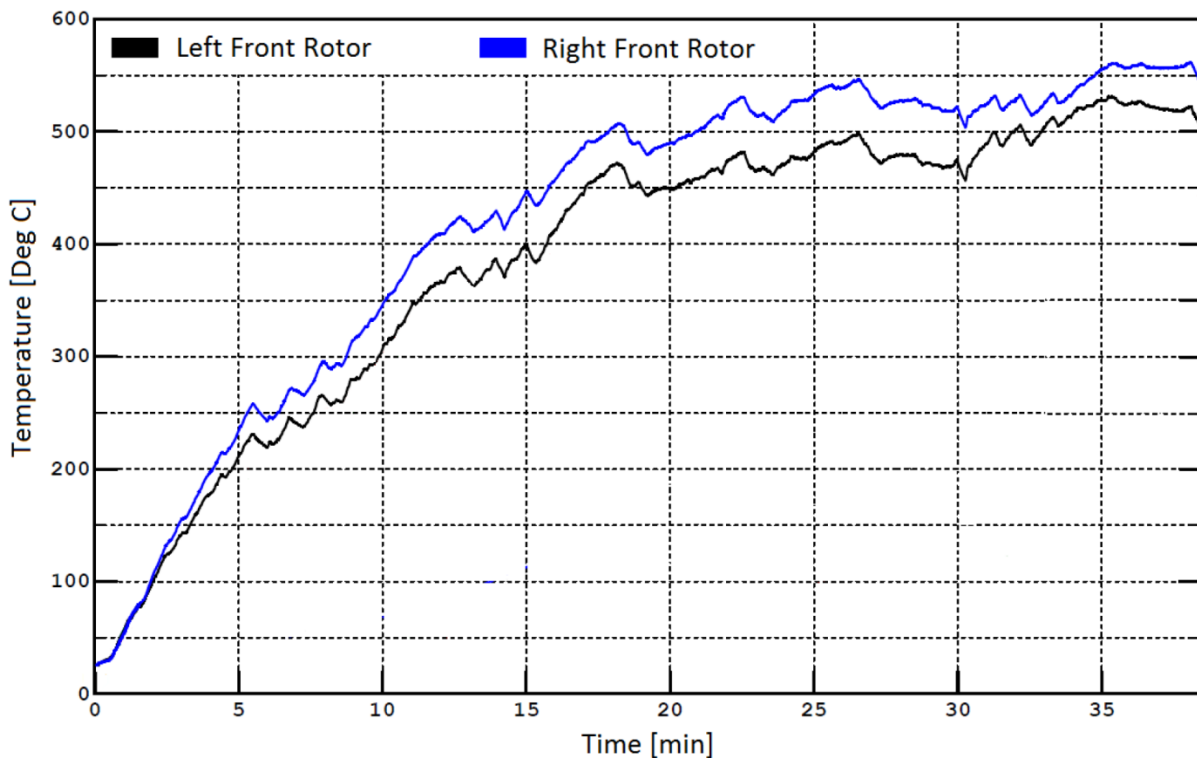


Figure 14: Temperature profiles for left and right rotors during a descent with the VW Tiguan. Right hand bias clearly can be seen.

## Future Work

Excessive or insufficient cooling over the course of the descent will have a significant effect upon the accuracy of the resulting data. A velocity-driven, dynamic convective cooling mechanism could be employed which would approximate the cooling on the different surfaces of the rotor. These differences would be largely governed by the airflow around the rotor which can be investigated using full-assembly modelling and CFD techniques. CFD studies from M Tirovic in (1) indicate that the convective heat transfer values differ from 4 to 40  $\text{Wm}^{-2}\text{K}^{-1}$ . The various surfaces of the rotor would be subjected to differing rates of heat transfer. These differences would be the result of the pumping action generated within the vanes, general flows across the rotor caused by vehicle motion and forced-airflow due to the revolutions.

To further test the adequacy of the methodology, the experimental procedure can be repeated with an array of other vehicles. This may lead to the acquisition of an alternative velocity profile that better suits all of the extant data, thus resulting in either the increased accuracy or the redundancy of the current profile. A more desirable approach may utilise a range of velocity profiles that are tailored to groups of vehicles categorised by mass. Multi-body FEA and thermo-tribological analysis using the appropriate frictional models are also some of the many other potentialities for further investigation. Experimental axle load measurements could be analysed and used to validate the theoretically proposed values for dynamic mass balance.

## References

- (1) Day A. J., "Braking of Road Vehicles", University of Bradford, 1st Ed, p260, 2005
- (2) Guiggiani M., "The Science of Vehicle Dynamics", Springer, p103, 2014
- (3) Limpert R., "Brake Design and Safety", SAE International, 3rd Ed, p66, 2011
- (4) Modest M., "Radiative Heat Transfer", Elsevier, p824, 2013
- (5) "Tiguan Vehicle Information", Volkswagen, URL <http://www.volkswagen.co.uk/new/tiguan-gp/which-model>, 2015
- (6) Andreescu C., Clenci A., "Proceedings of the European Automotive Congress EAEC-ESFA 2015", Springer, p308, 2015
- (7) Day A. J., "Braking of Road Vehicles", University of Bradford, 1st Ed, p223, 2005
- (8) Day A. J., "Braking of Road Vehicles", University of Bradford, 1st Ed, p256, 2005
- (9) Straffelini G., "Friction and Wear", Springer, p91, 2015